

## Supporting Information

Table S1. Bacterial colonization in wounds of patients with RDEB.

Table S2. Bacterial colonization of mouse skin.

Fig. S1. Splenic follicular conduits contain also other components of the dermal-epidermal junction zone adhesion complexes.

Fig. S2. Collagen VII is located in the basement membrane-associated microfibril layer in follicular conduits.

Fig. S3. Reduced abundance of cochlin in RDEB mouse forepaws.

Fig. S4. Increased aggrecanase-1 and -2 expression in spleen of RDEB mice.

Fig. S5. Co-expression of collagens IV and VII, but limited co-expression of collagens I and VII in spleen.

Fig. S6. Collagen VII and cochlin interact in solution.

Fig. S7 Expression of cochlin LCCL, VWFA1 and VWFA2 domains.

Fig. S8. Cochlin abundance is not reduced in cultured RDEB splenic stromal cells.

Fig. S9. Collagen VII promotes retention of cochlin in lymph nodes.

Fig. S10. The cochlin LCCL domain rapidly evokes tyrosine phosphorylation of selective protein in the murine macrophage cell line RAW 264.7.

Fig. S11. Intraperitoneally injected human recombinant collagen VII deposits in spleen but not in skin.

References

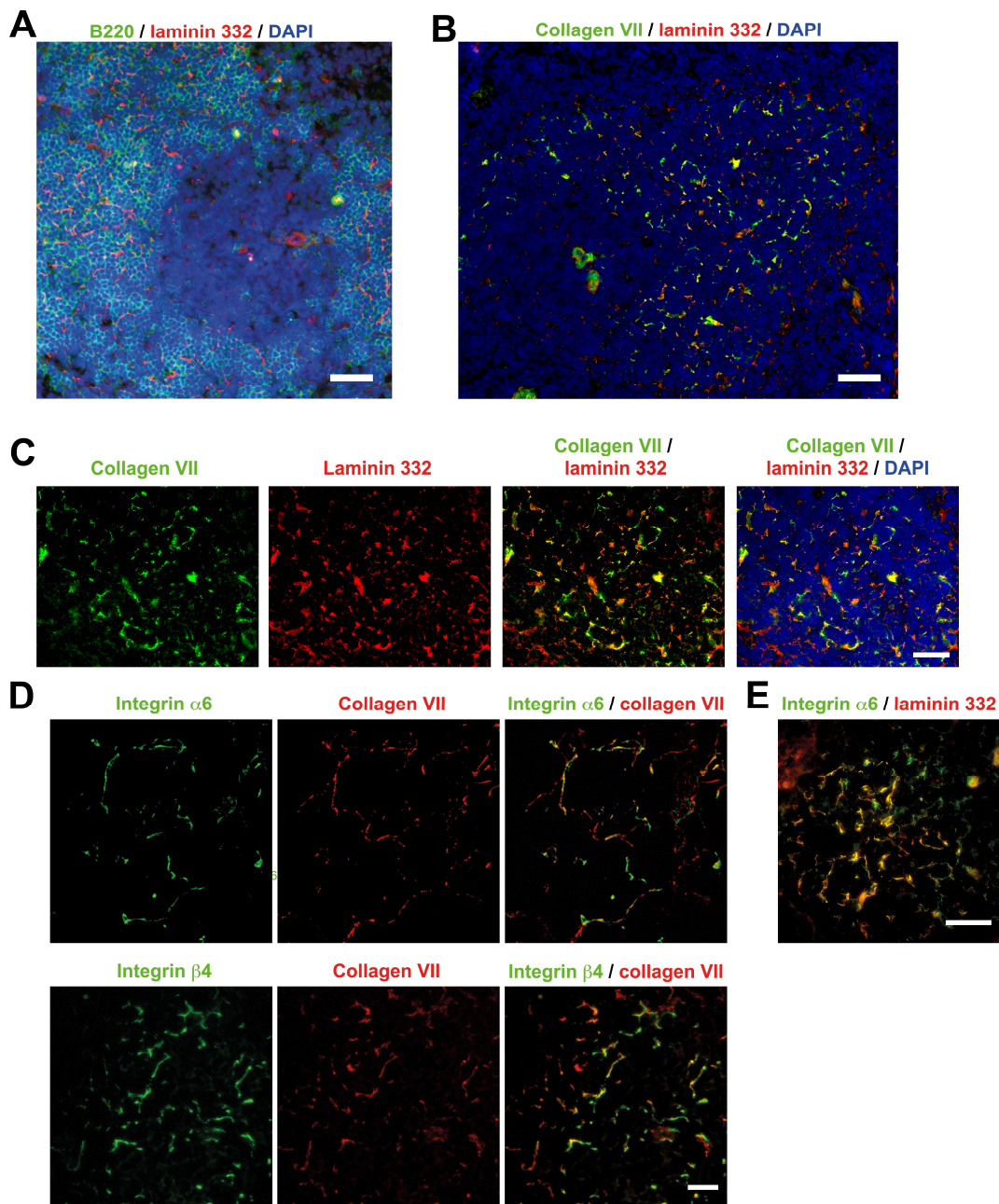
**Table S1: Bacterial colonization in wounds of patients with RDEB.**

Patient	Gender	Age	Bacteria / fungus on skin swabs
1	M	3	<i>Staphylococcus aureus</i>
2	M	7	<i>Staphylococcus aureus</i> , <i>Pseudomonas aeruginosa</i> , <i>Streptococcus sp.</i>
3	M	8	<i>Staphylococcus aureus</i> , <i>Proteus mirabilis</i>
4	M	11	<i>Staphylococcus aureus</i> , <i>Pseudomonas aeruginosa</i> , <i>Streptococcus sp.</i> , <i>Proteus mirabilis</i>
5	M	11	<i>Staphylococcus aureus</i>
6	F	15	<i>Staphylococcus aureus</i> , <i>Streptococcus sp.</i> , Methicillin-resistant <i>Staphylococcus aureus</i>
7	M	17	<i>Staphylococcus aureus</i> , <i>Pseudomonas aeruginosa</i> ,
8	M	17	<i>Staphylococcus aureus</i>
9	F	18	<i>Staphylococcus aureus</i>
10	F	19	<i>Staphylococcus aureus</i> , <i>Streptococcus sp.</i> , <i>Corynebacteria</i>
11	M	20	<i>Staphylococcus aureus</i>
12	M	20	<i>Staphylococcus aureus</i> , <i>Proteus mirabilis</i>
13	M	20	<i>Staphylococcus aureus</i> , <i>Pseudomonas aeruginosa</i>
14	F	21	<i>Staphylococcus aureus</i> , <i>Streptococcus sp.</i> , <i>Klebsiella oxytoca</i>
15	F	21	<i>Staphylococcus aureus</i> , <i>Streptococcus sp.</i> , Methicillin-resistant <i>Staphylococcus aureus</i>
16	M	21	<i>Staphylococcus aureus</i> , <i>Pseudomonas aeruginosa</i> , <i>Proteus mirabilis</i> , <i>Klebsiella oxytoca</i>
17	M	22	<i>Staphylococcus aureus</i> , <i>Pseudomonas aeruginosa</i> , <i>Streptococcus sp.</i> , <i>Candida tropicalis</i> , <i>Serratia marcescens</i> , <i>Klebsiella ozaenae</i>
18	M	23	<i>Staphylococcus aureus</i> , <i>Pseudomonas aeruginosa</i> , <i>Streptococcus sp.</i>
19	F	25	<i>Staphylococcus aureus</i> , <i>Streptococcus sp.</i>
20	M	26	<i>Staphylococcus aureus</i>
21	F	29	<i>Staphylococcus aureus</i> , <i>Pseudomonas aeruginosa</i> , <i>Streptococcus sp.</i>

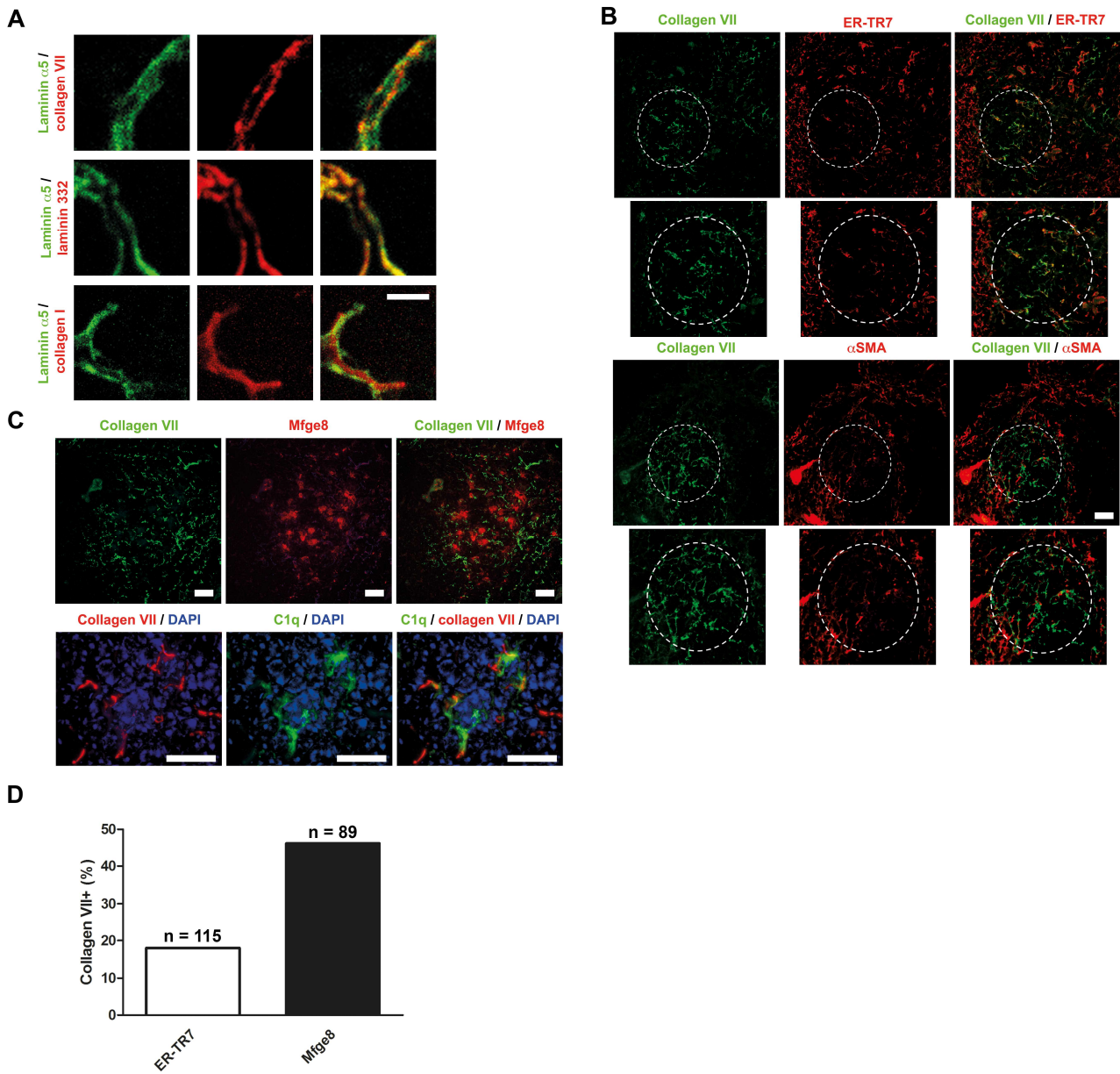
22	M	31	<i>Staphylococcus aureus, Streptococcus sp.</i>
23	M	31	<i>Staphylococcus aureus</i>
24	M	33	<i>Staphylococcus aureus, Streptococcus sp., Proteus mirabilis</i>
25	M	34	<i>Staphylococcus aureus, Pseudomonas aeruginosa, Candida albicans, Enterobacter cloacae, Corynebacteria</i>
26	M	34	<i>Staphylococcus aureus</i>
27	M	35	<i>Staphylococcus aureus</i>
28	M	41	<i>Staphylococcus aureus, Pseudomonas aeruginosa, Streptococcus sp. Proteus mirabilis</i>
29	F	53	<i>Staphylococcus aureus, Pseudomonas aeruginosa, Proteus mirabilis,</i>
30	M	67	<i>Staphylococcus aureus, Streptococcus sp., Candida albicans</i>

**Table S2: Bacterial colonization on mouse skin****Nr. Gender Genotype Age (wk) Bacteria on skin swabs**

Nr.	Gender	Genotype	Age (wk)	Bacteria on skin swabs
1	F	Wild-type	6	-
2	F	Wild-type	6	-
3	M	Wild-type	7	-
4	F	RDEB	6	<i>Staphylococcus aureus</i> , <i>Streptococcus sp.</i>
5	F	RDEB	6	<i>Staphylococcus aureus</i> , <i>Streptococcus sp.</i>
6	M	RDEB	7	<i>Staphylococcus aureus</i> , <i>Streptococcus sp.</i>
7	F	Wild-type	10	-
8	M	Wild-type	10	<i>Streptococcus sp.</i> , <i>Rothia nasimurium</i>
9	F	Wild-type	10	-
10	M	Wild-type	10	<i>Streptococcus sp.</i> , <i>Rothia nasimurium</i>
11	F	Wild-type	10	-
12	F	RDEB	10	<i>Staphylococcus aureus</i> , <i>Streptococcus sp.</i> , <i>Staphylococcus xylosum</i> , <i>Lactococcus lactis</i> ,
13	M	RDEB	10	<i>Staphylococcus aureus</i> , <i>Streptococcus sp.</i> , <i>Staphylococcus xylosum</i> , <i>Aerococcus viridans</i> , <i>Enterococcus faecalis</i>
14	F	RDEB	10	<i>Staphylococcus aureus</i> , <i>Streptococcus sp.</i> , <i>Enterobacter cloacae</i> , <i>Acinetobacter johnsonii</i>
15	M	Wild-type	22	<i>Staphylococcus aureus</i> , <i>Streptococcus sp.</i>
16	M	RDEB	22	<i>Staphylococcus aureus</i> , <i>Klebsiella oxytoca</i>

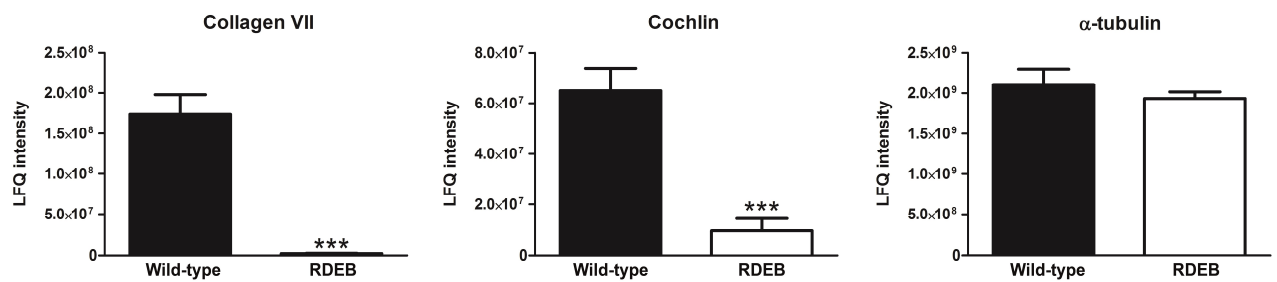


**Fig. S1** Splenic follicular conduits contain also other components of the dermal-epidermal junction zone adhesion complexes. **(A)** Spleen stained for B220 (green) and laminin 332 (red), nuclei visualized with DAPI. **(B)** Sections stained for collagen VII (green) and laminin 332 (red), and nuclei visualized with DAPI. Scale bars in A and B = 100  $\mu\text{m}$ . **(C)**, Higher magnification and presentation of individual channels of stainings as in (B). (B-C) Note the similar distribution of laminin 332 and collagen VII in spleen. **(C)** Splenic follicle stained for integrin  $\alpha 6$  and  $\beta 4$  (green), and collagen VII (red). **(D)** Splenic follicle stained for integrin  $\alpha 6$  and laminin 332 (red). Scale bars in C, D and E = 50  $\mu\text{m}$ .



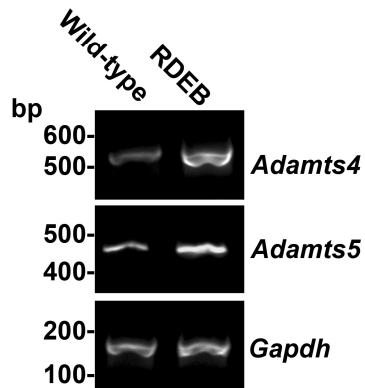
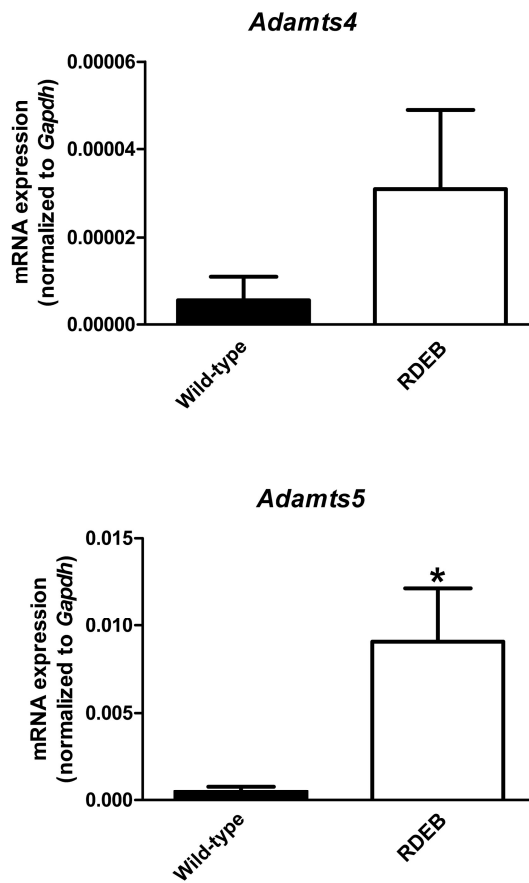
**Fig. S2** Collagen VII is located in the basement membrane-associated microfibril layer in follicular conduits. **(A)** Single-plane confocal image of splenic conduits stained for laminin  $\alpha 5$  (green) and collagen VII, laminin 332 and collagen I (all red), as indicated. In the top and middle panels follicular conduits are shown and in the bottom panel T cell zone conduits are shown. Note the close co-localization between laminin  $\alpha 5$  and laminin 332, the close but not overlapping staining of laminin  $\alpha 5$  and collagen VII, and a clearly visible collagen core in T cell zone conduits in the co-staining with collagen I and laminin  $\alpha 5$ . Scale bar = 10  $\mu\text{m}$ . **(B)** Splenic white pulp co-stained for collagen VII (green) and the T cell zone conduit marker ER-TR7 (red)

or the FRC marker  $\alpha$ SMA (red). There is limited co-distribution of ER-TR7 and  $\alpha$ SMA with collagen VII, as indicated in the selected areas (dotted line). Lower panel shows magnification of parts of the upper panel. **(C)** Sections as in (B) co-stained with collagen VII (green or red) and the FDC markers Mfge8 (red) and C1q (green). Scale bars = 10  $\mu$ m, nuclei visualized with DAPI (blue). In spleen collagen VII shows close association with both FDC markers. **(D)** Quantification of the percentage of collagen VII positive conduits that also was positive for ER-TR7 and Mfge8. Indicated in the figure is the number of conduits analyzed per staining. The conduits were quantified using Image J. The quantification supports the visual impression of more collagen VII staining in FDC positive areas than areas where ER-TR7 – predominantly a T cell conduit marker – is present.



**Fig. S3** Reduced abundance of cochlin in RDEB mouse forepaws. Whole forepaw protein lysates from adult wild-type and RDEB mice ( $n = 6$ ), were analyzed by label-free proteomics. Bar graphs show the abundance of collagen VII, cochlin and  $\alpha$ -tubulin (tubulin alpha-1A chain; tubulin alpha-3 chain) to ensure equal loading. The values represent mean  $\pm$  S.E.M of the normalized protein abundance (LFQ intensity). Collagen VII wild-type vs. RDEB \*\*\* $P = 0.0009$  (unpaired t-test with Welch's correction); cochlin wild-type vs. RDEB \*\*\* $P = 0.0003$  (unpaired t-test) and  $\alpha$ -tubulin wild-type vs. RDEB  $P = 0.42$ .



**A****B**

**Fig. S4** Increased aggrecanase-1 and -2 expression in spleen of RDEB mice. **(A)** Representative RT-PCR after 40 cycles of mRNA extracted from 10-week-old wild-type and RDEB mouse spleens. Shown are the products of the for *Adamts4* gene encoding aggrecanase-1, *Adamts5* gene encoding aggrecanase-2, and the housekeeping gene *Gapdh*. **(B)** qRT-PCR of mRNA extracted from spleens as in (A). mRNA expression normalized to *Gapdh*. *Adamts4* expression did not reach statistical significance due to variation of expression in the RDEB mouse spleens. *Adamts5* is significantly increased in RDEB, \* $P = 0.023$ ,  $n = 4$ , significance tested with unpaired Student's *t*-test.

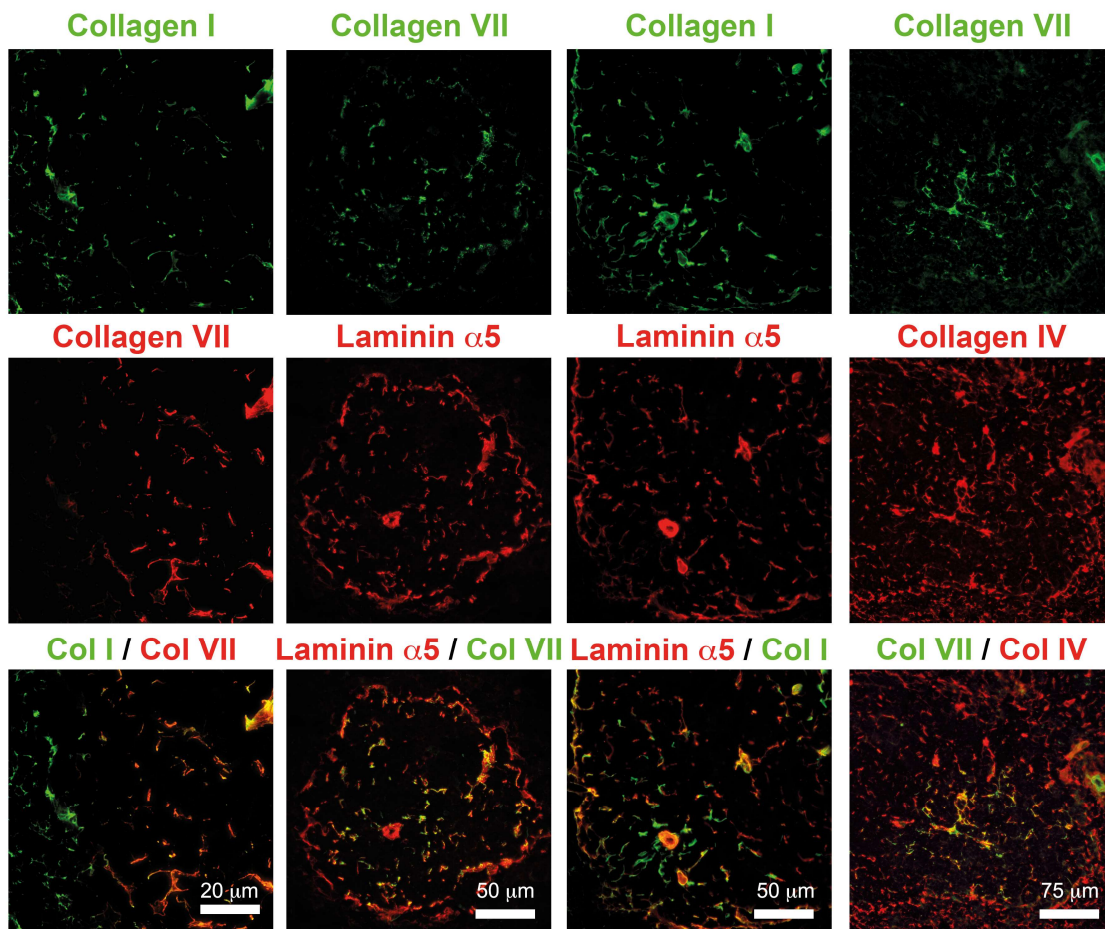


**Fig. S5** Co-expression of collagens IV and VII but limited co-expression of collagens I and VII in spleen. Left panel, splenic white pulp stained for collagen I (green) and collagen VII (red) or middle panels stained for collagen I (green), collagen VII (green) and laminin  $\alpha 5$  (red). Note the limited overlap of collagen I and VII expression, both in the double staining and in the stainings using laminin  $\alpha 5$  as positional reference. Right panel, co-staining of collagen VII (green) and collagen IV (red). Note the broader distribution of collagen IV but with good co-localization with collagen VII in areas where collagen VII is present. Scale bars = 20  $\mu\text{m}$ , 50  $\mu\text{m}$  and 75  $\mu\text{m}$ , as indicated in the panels.

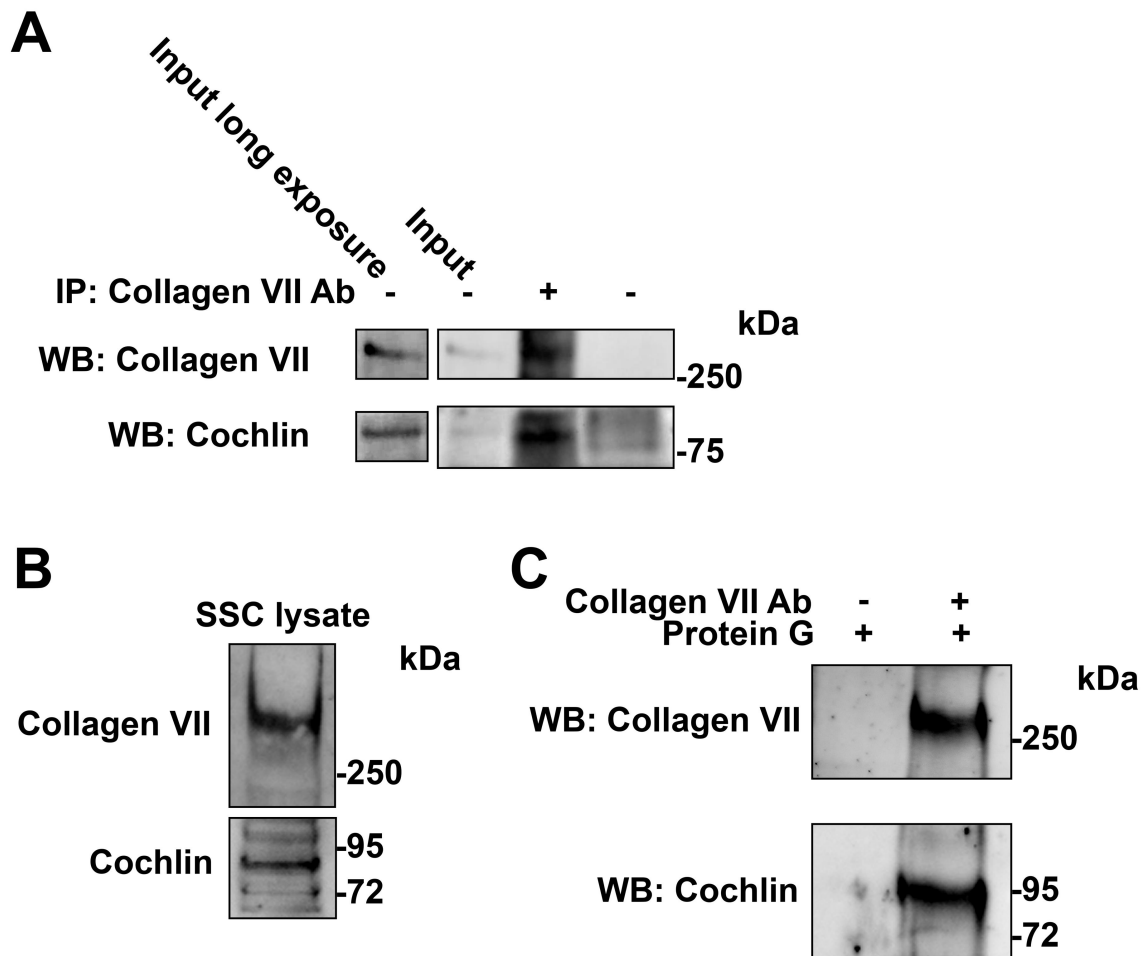


**Fig. S6** Collagen VII and cochlin interact in spleen and in solution. **(A)** Immunoprecipitation (IP) using collagen VII antibodies or non-immune rabbit serum on spleen lysates from wild-type mice. Blots probed for collagen VII (Col VII) and cochlin. **(B)** Western blot of lysates of cultured splenic stromal cells (SSC) showing that the cells express both collagen VII and cochlin. **(C)** Interaction of collagen VII and cochlin in SSC-conditioned medium. SSC-conditioned medium was precipitated with either collagen VII antibodies bound to Protein G sepharose beads or with Protein G sepharose beads alone. The precipitates were analysed by western blots for collagen VII or cochlin as indicated.

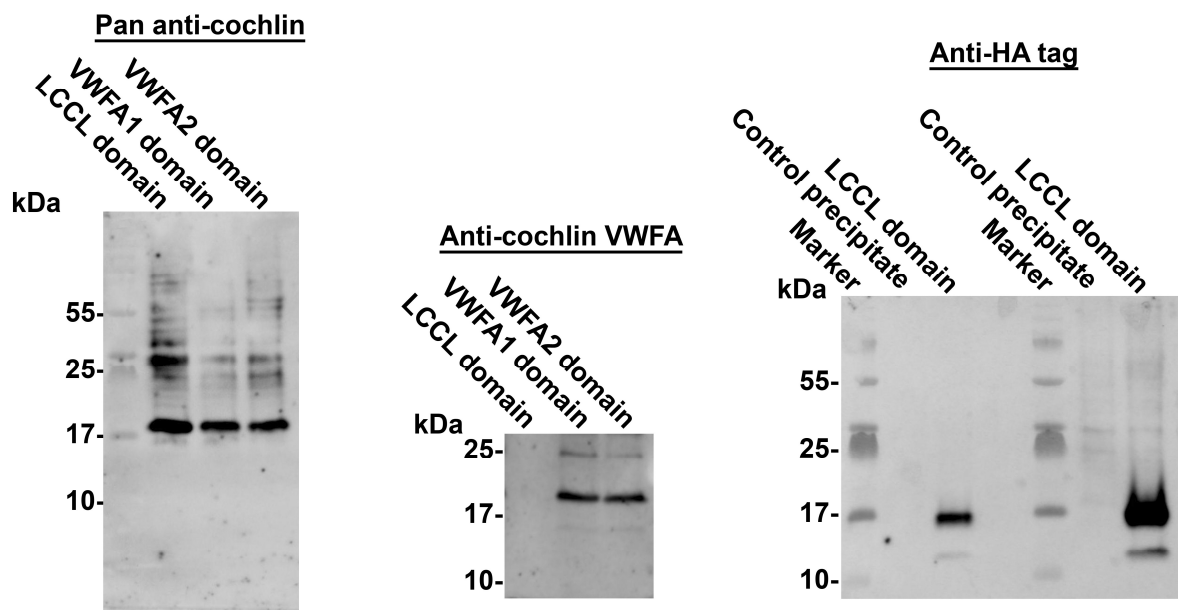


**Fig. S7** Expression of cochlin LCCL, VWFA1 and VWFA2 domains. Conditioned medium from HEK-293 cells precipitated with 80% saturated ammonium sulfate analyzed by western blotting by antibodies detecting all domains of cochlin (left), the VWFA domains only (middle) or the HA-tag of the LCCL domain (right). In the right blot 10  $\mu$ l and 30  $\mu$ l of the precipitates were loaded. Control precipitate was from conditioned medium of untransfected HEK-293 cells. The two bands of the LCCL domain bands correspond to glycosylated (major) and unglycosylated (minor) LCCL domain (1).

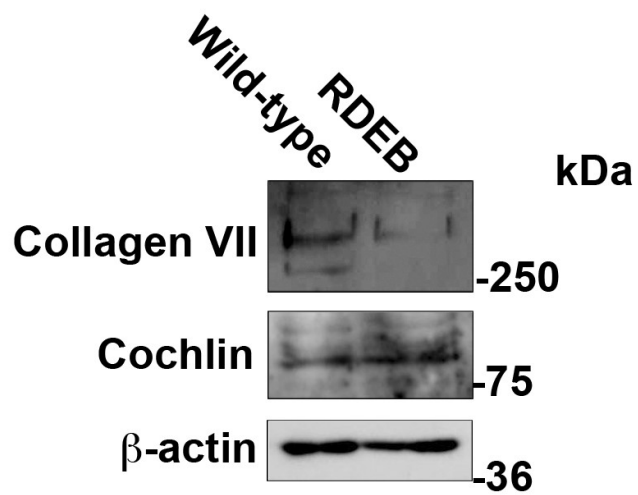


**Fig. S8** Cochlin abundance is not reduced in cultured RDEB splenic stromal cells. Western blots of protein lysates from splenic stromal cells isolated from 8-week-old wild-type and RDEB mice. The blot was probed for collagen VII, cochlin (rat monoclonal antibody clone 9A10D2) and  $\beta$ -actin to ensure equal loading. The blot reveals similar levels of cochlin in wild-type and RDEB splenic stromal cells.

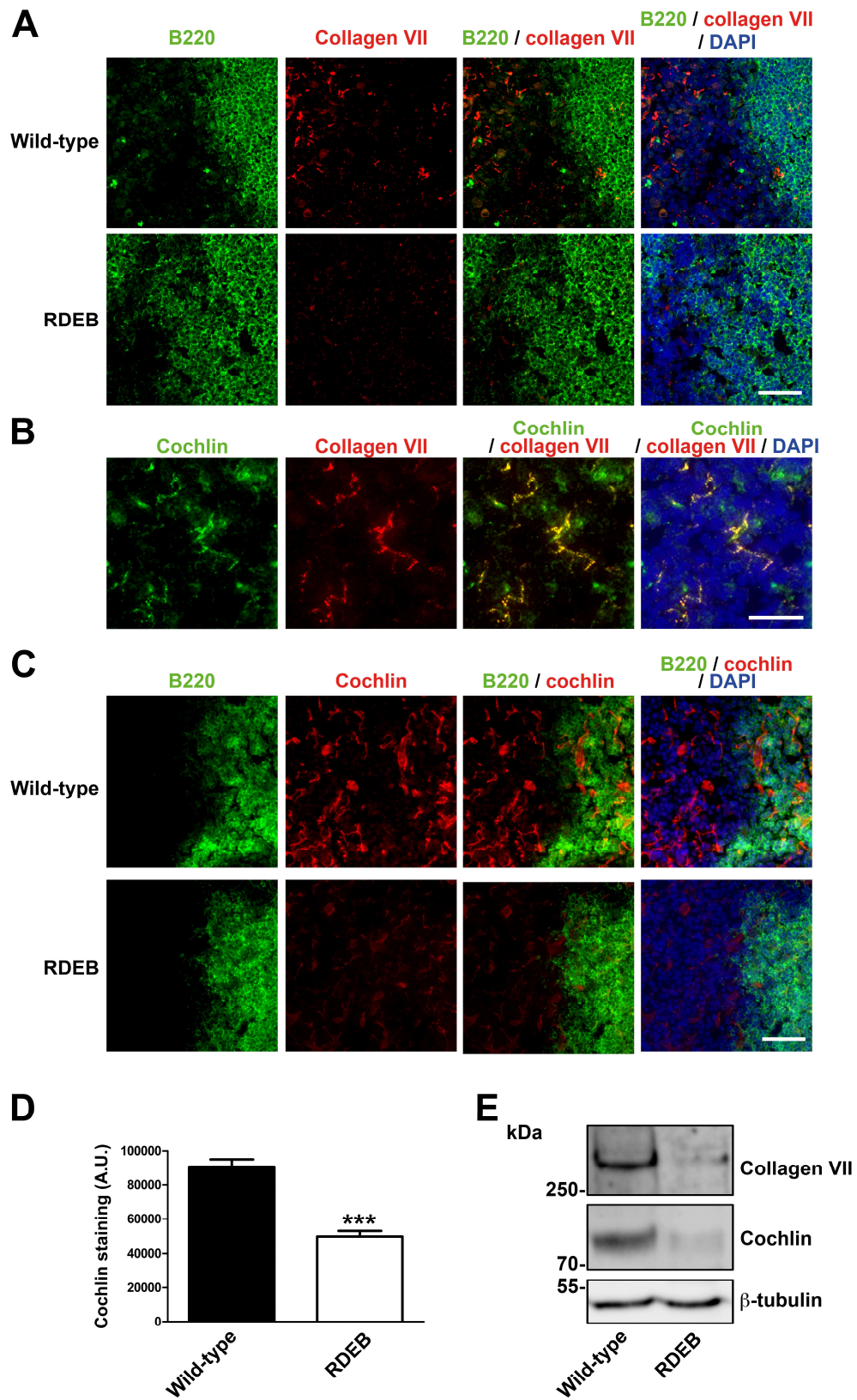


**Fig. S9** Collagen VII promotes retention of cochlin in lymph nodes. Mandibular lymph nodes from 10-week-old wild-type and RDEB mice stained for: **(A)** B cells (B220, green) and collagen VII (red); nuclei visualized with DAPI (blue). Scale bar = 100  $\mu$ m. **(B)** Co-staining with cochlin

(goat polyclonal, green) and collagen VII (red); nuclei visualized with DAPI (blue). Scale bar = 50  $\mu\text{m}$ . **(C)** B cells (B220, green) and cochlin (rabbit polyclonal, red); nuclei visualized with DAPI (blue). Scale bar = 100  $\mu\text{m}$ . Importantly, in lymph nodes both collagen VII and cochlin display a wider distribution than in spleen and are present both in B cell areas outside these areas. **(D)** Quantification of the immunofluorescence staining intensity of stainings as in (C);  $n = 4$ , values represent mean  $\pm$  S.E.M,  $***P < 0.0001$ . **(E)** Western blot on whole mandibular lymph node protein extracts from 10-week-old wild-type and RDEB mice. The blots were probed for collagen VII, cochlin (rat monoclonal, clone 9A10D2) and  $\beta$ -tubulin to ensure equal loading. In total four wild-type and four RDEB lymph nodes were analyzed, of which three RDEB lymph nodes showed significant reduction in cochlin.

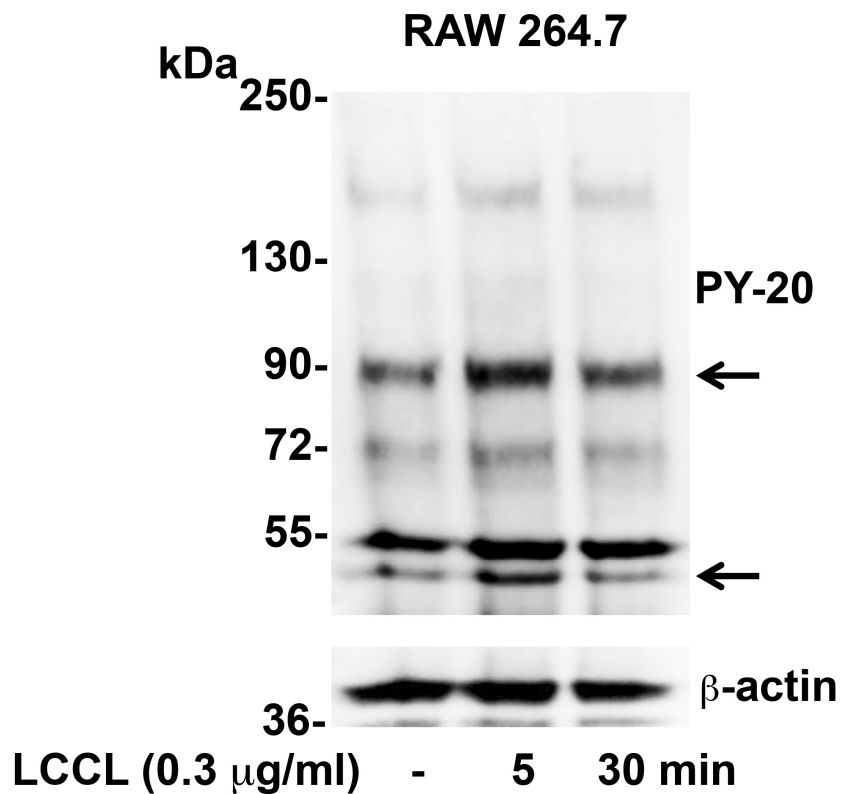


**Fig. S10** The cochlin LCCL domain rapidly evokes tyrosine phosphorylation of selective proteins in the murine macrophage cell line RAW 264.7. Serum starved RAW 264.7 cells treated with 0.3 µg/ml recombinant murine cochlin LCCL domain for 5 or 30 min. Protein lysates were analyzed by western blotting for tyrosine phosphorylation using the pan-phospho-tyrosine antibody PY20. β-actin used as loading control. Note the distinct rapid and transient phosphorylation of 90 kDa and 50 kDa sized protein (arrows).



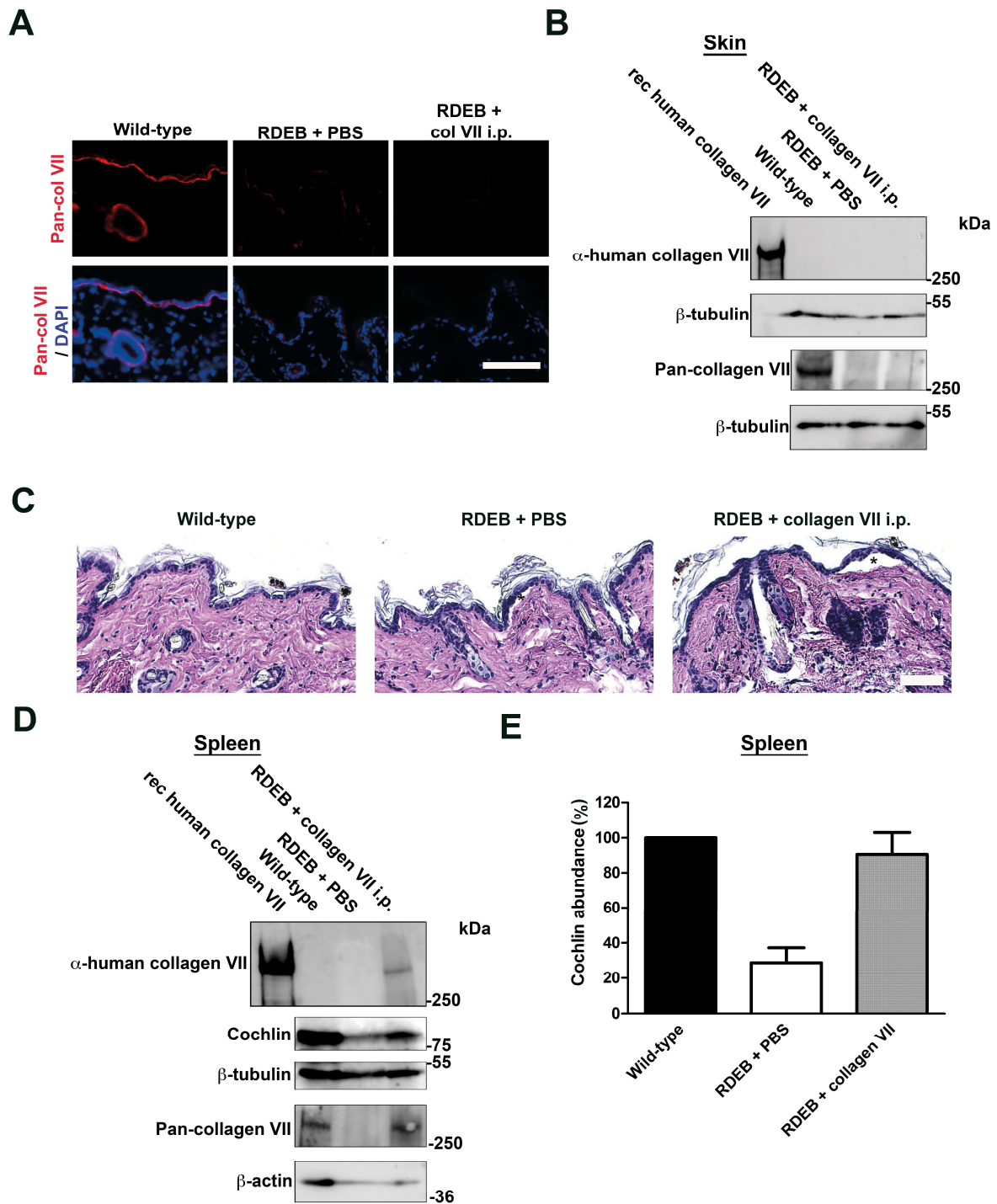


**Fig. S11** Intraperitoneally injected human recombinant collagen VII deposits in spleen but not in skin. **(A)** Staining of back skin from wild-type mice or RDEB mice one-week after intraperitoneal injections with PBS or human recombinant collagen VII as indicated, with an antibody detecting both murine and human collagen VII (Pan-Col VII (red)). Nuclei visualized with DAPI, scale bar = 50  $\mu$ m. **(B)** Western blotting of protein lysates of whole back skin from mice presented in (A).

Blots probed for antibodies specific for human collagen VII (2) or detecting both murine and human collagen VII (Pan-collagen VII).  $\beta$ -tubulin used as loading control. Recombinant human collagen VII was run as a control for reactivity of the human collagen VII specific antibody (C) H&E stained sections of paraffin-embedded back skin from a wild-type mouse (left panel) and an RDEB mouse injected with PBS (middle panel) and 20  $\mu$ g human recombinant collagen VII (right panel). Note that skin blistering (asterisk) still occurs after collagen VII injection, indicating that intraperitoneally injected collagen VII do not promote systemic skin stabilization. Scale bar = 50  $\mu$ m. (D) Western blots of protein lysates from whole spleen from mice in A and B. Blots were probed with antibodies specific for human collagen VII (2), cochlin (rabbit antibody), detecting both human and murine collagen VII (Pan-collagen VII).  $\beta$ -tubulin and  $\beta$ -actin were used as loading controls. (E) Quantification of cochlin abundance in spleen from mice treated as in (A, B and D). Values represent mean  $\pm$  S.E.M, \*P = 0.0261 (WT vs. RDEB + PBS) and 0.0253 (RDEB + collagen VII vs. RDEB + PBS); n = 4. Note that intraperitoneally injected human collagen VII is not detectable in RDEB mouse skin but is clearly present in spleen and that this treatment results in normalization of splenic cochlin levels.

## References

1. Py BF, et al. (2013) Cochlin produced by follicular dendritic cells promotes antibacterial innate immunity. *Immunity* 38(5):1063–1072.
2. Kühl T, et al. (2015) High Local Concentrations of Intra-dermal MSCs Restore Skin Integrity and Facilitate Wound Healing in Dystrophic Epidermolysis Bullosa. *Mol Ther J Am Soc Gene Ther* 23(8):1368–1379.